LAWRENCE
LIVERMORE
NATIONAL
LABORATORY

LLNL-JRNL-584312

Carbon Turnover in Water-Soluble Protein of the Adult Human Lens

D. N. Stewart, J. Lango, K. P. Nambiar, M. J. S. Falso, P. G. FitzGerald, D. M. Rocke, B. D. Hammock, B. A. Buchholz

September 24, 2012

Molecular Vision

Disclaimer

Carbon Turnover in Water-Soluble Protein of the Adult Human Lens

Daniel N. Stewart[1], Jozsef Lango[1], Krishnan P. Nambiar[1], Miranda J. S. Falso[2,6], Paul G. FitzGerald[3], David M. Rocke[4], Bruce D. Hammock[5], and Bruce A. Buchholz[2]*

[1]Department of Chemistry, University of California, One Shields Avenue, Davis, CA 95616 USA.

[2]Center for Accelerator Mass Spectrometry, Lawrence Livermore National Laboratory, 7000 East Avenue, Livermore, CA 94551 USA

[3]Department of Cell Biology and Human Anatomy, School of Medicine, University of California, Davis, CA 95616 USA.

[4]Division of Biostatistics, School of Medicine, University of California, Davis, CA 95616 USA.

[5]Department of Entomology and Comprehensive Cancer Center, University of California, One Shields Avenue, Davis, CA 95616 USA.

[6]Currently Division of Math and Sciences, Pennsylvania State University – Altoona, Altoona, PA 16601 USA

*Address correspondence to

Bruce Buchholz, Ph.D., Center for Accelerator Mass Spectrometry, Lawrence Livermore National Laboratory, Mail stop L-397, P.O. Box 808, 7000 East Avenue, Livermore, CA 94551-9900 Phone: +1-925-422-1739, FAX: +1-925-423-7884, email: buchholz2@llnl.gov

Abstract

Purpose: Human eye lenses contain cells that persist from embryonic development. These unique, highly specialized fiber cells located at the core (nucleus) of the lens undergo pseudo-apoptosis to become devoid of cell nuclei and most organelles. Ostensibly lacking in protein transcriptional capability, it is currently believed these nuclear fiber cells owe their extreme longevity to the perseverance of highly stable and densely packed crystallin proteins. Maintaining the structural and functional integrity of lenticular proteins is necessary for sustaining cellular transparency and proper vision, yet the means by which the lens actually copes with a lifetime of oxidative stress, seemingly without any capacity for protein turnover and repair, is not completely understood. Although many years of research have been predicated upon the assumption that there is no protein turnover or renewal in nuclear fiber cells, we investigated whether different protein fractions possess protein of different ages by using the ^{14}C bomb pulse. Methods: Adult human lenses were concentrically dissected by gently removing cell layers in water or shaving to the nucleus with a curved micrometer controlled blade. Cells were lysed and proteins were separated into water-soluble and water-insoluble fractions. Small molecules were removed by the use of 3 kDa spin filters. The $^{14}C/C$ was measured in paired protein fractions by accelerator mass spectrometry and an average age for the material within the sample was assigned using the ^{14}C bomb pulse. Results: The water-insoluble fractions possessed $^{14}C/C$ ratios consistent with the age of the cells. The water-soluble fractions contained carbon younger than the paired water-insoluble fraction in all cases. Conclusion: As the first direct evidence for carbon turnover in protein from adult human nuclear fiber cells, this discovery supports the emerging view of the lens nucleus as a dynamic system capable of maintaining homeostasis in part by an intricate protein transport mechanisms and

possibly by protein repair. This finding implies that the lens plays an active role in the aversion of age related nuclear (ARN) cataract.

Keywords

Age related nuclear cataracts; carbon bomb-pulse dating; crystallin; protein renewal

1. Introduction

The overall structure of the human lens is one of successive generations of secondary fiber cells stratified chronologically around the embryonic nucleus, the primary fiber cells formed by week six after fertilization [1,2]. Because all cells are retained, the lens grows continuously throughout life, and its history is well preserved within the tissue.

The formation of age-related nuclear (ARN) cataracts is associated with aging of the lens and characterized by the loss of optical transparency [3]. Age is the single largest risk factor for ARN cataract; however there are clear distinctions between the protein alterations brought on by the ageing process and those associated with cataract formation [4-10]. ARN cataracts are typically associated with oxidative stress causing conformational changes, aggregation, and loss of solubility of the abundant, densely packed proteins of the lens fiber cells [1,3,4,11,12]. The lens must support the functionality of all its constituent cells for a lifetime, yet the manner by which it preserves homeostasis in its aged nuclear fiber cells is not fully understood. It is presumed that failure to preserve the viability of any fiber cell leads to pathology [11].

An “inner circulatory system” of ion channels, Na/K pumps, gap junctions, and water channels has been reported for the active transport of fluid, ions, and small

molecules between the superficial and innermost regions of the lens in order to maintain homeostasis [13-18]. Aquaporin-0 (AQP0), or membrane intrinsic protein (MIP), is the primary aquaporin expressed in the lens fibers. Aquaporins are integral membrane proteins with the main function of transporting water across cell membranes. Mutations in AQP0 have been shown to play a role in ARN cataract formation [19,20]. Compared to other aquaporins, AQP0 demonstrates low water permeability and has been proposed to play other roles that may relate to ARN cataract formation. A variety of age-related post-translational modifications have been identified on AQP0, but how these modifications pertain to the formation of ARN cataracts has not been determined [21]. A second group of membrane proteins, the connexins (Cx), interacts with AQP0 to form the fiber-to-fiber junctions [22]. Cataracts often develop as a secondary effect of type II diabetes, and when a cataract lens from one of these patients was examined, Cx were lacking from the lens and the AQP0 arrays were misformed leading to a breakdown of the lens microcirculation system in the lens and opacification [16,23]. Mutations to Cx are a common cause of hereditary cataracts [16]. AQP0 also acts as a scaffold protein that organizes γ-crystallins [24]. Crystallins are the major protein component of the lens, with α-crystallin acting as a molecular chaperone and scaffold protein, and β- and γ-crystallins as structural proteins [3]. A colloidal model of α- and γ-crystallin proteins demonstrated another proposed mechanism for the formation of ARN cataracts. A weak, short-range attraction between α- and γ-crystallins maintains the transparency of concentrated crystallin mixtures and changes in the magnitude of this interaction may contribute to the formation of ARN cataracts [25]. In addition, the aging lens may experience adhesion of α-, β- and γ-crystallins or fragments of them to cell membranes, which may contribute to loss in lens flexibility and inhibit membrane properties with aging [8,9]. These studies all demonstrate the necessity of a functional circulatory system in the lens in order to prevent cataract formation.

A correlation has been found between the extensive protein oxidation that is the hallmark of age related nuclear (ARN) cataract and the barriers to metabolite transport that develop between the cortical and nuclear regions of the lens in middle age [4,26]. In addition to the "inner circulatory system" described above for the transport of fluids, ions, and low molecular mass constituents, research investigating large molecule transport indicated a protein permeable pathway within the nuclei of chicken and mouse lenses and demonstrated how those nuclei behaved as a syncytium [27-29]. More than forty years ago it was shown the ^{35}S-methionine crossed the cortical boundary in rats and entered the lens nucleus, but autoradiography could not distinguish whether the ^{35}S-methionine was free or incorporated in lens crystallin proteins [30]. Possibly even more striking was the discovery of significant numbers of transcriptionally-capable fiber cells located below the cortical-nuclear barrier in an adult population of mice [28]. Although these studies have shown that protein generation and transport is possible in the mammalian lens, most researchers still tacitly assume that protein turnover is nonexistent in human nuclear fiber cells, for there have been no long term metabolic labelling studies to evaluate this phenomenon. Circumventing the time constraints and feasibility of performing such a lengthy trial involving human subjects, we describe a "retrospective tracer" study in which we determine carbon turnover in protein of aged cells without the need for the administration of chemical tracers to the subjects prior to the analysis.

Extensive above ground testing of nuclear weapons doubled the atmospheric level of ^{14}C between the mid 1950s and the implementation of the Limited Test Ban Treaty in 1963 (see Figure 1). This pulse rapidly and evenly distributed throughout the Earth's atmosphere as $^{14}CO_2$ [31,32]. Since the test ban, the atmospheric radiocarbon concentrations have been decreasing exponentially as atmospheric CO_2 mixes into large terrestrial and marine carbon reservoirs. Known as the "bomb pulse," this

phenomenon is well characterized with an extensive high-resolution record [33-37]. Atmospheric ^{14}C levels from the bomb pulse closely correlate with the ^{14}C fingerprint found within dietary components from that given year, and moreover, it was confirmed that the annual ^{14}C averages in food matched those found in human tissue [38]. In a literal sense, anyone alive during this era unwittingly took part in a long-term radiocarbon tracer study where clinically safe levels of ^{14}C were incorporated into all proteins, DNA, and cellular structures, thus enabling researchers the ability to date the synthesis of a variety of biomolecules [39-56]. In this study we determine the date of synthesis of water-soluble and –insoluble proteins from the eye lens to determine a rate of carbon turnover.

2. Materials and Methods

2.1 Human lens dissection

The study was reviewed by the Lawrence Livermore National Laboratory Institutional Review Board and determined to be exempt. Human eyes were obtained through the University of California Davis Donated Body Program and Sierra Eye and Tissue Donor Services of Sacramento, CA. A total of 16 lenses ranging in age from 42 to 83 years old were analyzed in this study. Eye globes were frozen immediately post mortem and remained frozen until the time of dissection. Lenses were carefully extracted from the eye globes and verified to be structurally intact. In lenses obtained before 2009, layers of fiber cells were removed incrementally from their chronologically stratified topology by employing a stirring technique [57-61]. Lenses were allowed to reach room temperature and then placed into a 250mL glass beaker with 100 mL DDH_2O and a small magnetic stir bar atop a magnetic stirring plate. The layers of cells were slowly peeled away concentrically in the stirred water. Visual inspection was used to determine when enough cells were removed to yield sufficient carbon for isotope analysis. All the water

containing the peeled cells was removed by pipette, along with two small rinses of DDH_2O. The remaining portion of lens was carefully transferred to a second 250mL beaker containing a clean stir bar and 100 mL of fresh DDH_2O. The process was repeated until the entire lens had peeled into the water. Lenses obtained after 2009 were frozen in LN and shaved from the outside toward the center until the nucleus was reached. The innermost slices (~ 500 μm) were collected and analysed. The center slices primarily consisted of the lens nucleus, although the edge of the slices contained some younger cells. Isolated fiber cells were lysed by freeze/thaw cycles and centrifuged at 20,000g for 30 min at 4°C to separate the water-soluble and water-insoluble components of the cells. Samples processed after 2009 were further purified using molecular weight spin filters (Sartorius Vivaspin 3000 MWCO) to remove small molecules. Filters were initially rinsed with 5 mL of 18.2 MΩ water to remove preservative from filters and then samples were loaded onto filters following manufacturer's directions. Samples were rinsed an additional 3-5 times with 18.2 MΩ water to remove residual small molecules. Samples were concentrated to less than 500 μL for ^{14}C analysis.

2.2 ^{14}C analysis

Isolated fractions of water-soluble and water-insoluble proteins were analyzed for $^{14}C/C$ concentration by accelerator mass spectrometry (AMS). All AMS analyses were performed blind to age and origin of the sample. Water-soluble and water-insoluble protein fractions were lyophilized to dryness and transferred to quartz combustion tubes. NIST SRM 4990C (Oxalic Acid II) and IAEA C-6 (sucrose) were dissolved in water and co-lyophilized with the samples as controls to monitor carbon contamination during drying. Excess copper oxide (CuO) was added to each dry sample, and the tubes were brought to vacuum with a turbo pump station and sealed with a H_2/O_2 torch. Tubes were placed in a furnace set at 900°C for 3.5 h to combust all carbon to carbon

dioxide (CO_2). The evolved CO_2 was purified, trapped, and reduced to graphite in the presence of iron catalyst in individual reactors [62,63]. All $^{14}C/C$ measurements were completed with graphite targets analyzed at the Center for Accelerator Mass Spectrometry at Lawrence Livermore National Laboratory on the HVEE FN-class AMS system.

A $\delta^{13}C$ fractionation correction of –20±2 was used for all samples based on the measurements of selected sample splits of large CO_2 samples. Corrections for background contamination introduced during sample preparation were made following standard procedures [64]. All data were normalized with six identically prepared NIST SRM 4990B (Oxalic Acid I) standards. We used NIST SRM 4990C, IAEA C-6, and TIRI wood [65] as quality control secondary standards to monitor spectrometer performance. The measurement error was determined for each sample and ranged between ±2-10‰ (1 s.d.).

$^{14}C/C$ concentrations are reported using the $F^{14}C$ nomenclature for reporting post-bomb data defined in Eq. 2 of Reimer et al. (2004) [66]. It is enrichment or depletion of ^{14}C relative to oxalic acid standard normalized for isotope fractionation. All ^{14}C data in Tables 1 and 2 are reported as $F^{14}C$ and decay corrected $\Delta^{14}C$ following the convention of Stuiver and Polach (1977) [67]. This convention established for reporting radiocarbon data in chronological and geophysical studies was not developed to deal with post-bomb data. $\Delta^{14}C$ was calculated using the following formula:

$$\Delta^{14}C = 1000 * \{F^{14}C * \exp[\lambda*(1950 - y)] - 1\} \quad (1)$$

where $\lambda = 1/8267\ yr^{-1}$. y = year of measurement after 1950 A.D.

2.3 Protein identification of water insoluble fractions

Water insoluble protein samples were suspended in Rapigest (Waters, Bedford, MA, USA), reduced and alkylated according to Rapigest standard protocol, and digested with sequencing grade trypsin per the manufacturer's recommendations (Promega, Madison, WI). Protein identification was performed using a Paradigm LC system (Michrom Bioresources, Inc., Auburn, CA) coupled to an LTQ ion trap mass spectrometer (Thermo-Fisher, San Jose CA) through a Michrom nano-spray source. Peptides were loaded on to a Michrom nano trap and were then eluted and separated by a Michrom 0.2 x 150 mm column packed with Michrom Magic C18 reverse phase material (Michrom Bioresources, Inc., Auburn, CA). Peptides were eluted using a 70-minute gradient of 2-80% solvent B (buffer A = 99.9v% DI water and 0.1v% formic acid, solvent B = 95v% acetonitrile, 4.9v% DI water, 0.1v% formic acid) at flow rate of 2 µL/min. The top 10 ions in each survey scan were subjected to automatic low energy collision-induced dissociation (CID).

For database searching, product mode MS/MS spectra were extracted and charge state deconvoluted by BioWorks version 3.3 (Thermo-Fisher, San Jose CA). Deconvoluted MS/MS spectra were analyzed using X! Tandem software (www.thegpm.org; version 2006.04.01.2). For fragment recognition Iodoacetamide derivative of cysteine was specified in Mascot and X! Tandem as a fixed modification, oxidation of methionine was specified as a variable modification.

2.4 Protein identification of water soluble fractions

Protein samples were dissolved in Milli-Q water, and then filtered with Whatman 0.45 µm NYL filter (Whatman Inc., NJ, USA). Protein identification was performed based on the exact molecular mass measurements using high-resolution liquid chromatography-mass spectrometry (HR LC/MS) data. Exact mass measurement experiments were performed in positive ion mode on a Micromass/Waters LCT, an orthogonal

acceleration-Time-of-Flight (oa-TOF) mass spectrometer (Micromass, Manchester, UK) configured with a dual sprayer electrospray ion source, a standard Z-spray electrospray (ES) ionization source, and a lock-spray source that samples analyte and reference ions independently. The output analogue signal was digitalized using a 4 GHz time-to-digital converter (TDC).

A Waters Alliance 2795 (Bedford, MA, USA) high performance liquid chromatography (HPLC) system equipped with a Magic C18, 5 µm, 2.0x150 mm column (901-61221-00), (Michrom Bioresources, Inc., Auburn, CA) was used for sampling and solvent delivery. The column was equilibrated for 4 min with 100% solvent A at ambient temperature using a flow rate of 0.350 mL/min. The mobile phase used the following gradients: 0 min., 100% A; 5 min, 60 % B; 25 min, 100% B; 25-30 100% B. Mobile phase solvents expressed in volume % were the following: A: DI Water 99.9%, Trifluoroacetic acid 0.1%, (Sigma-Aldrich, spectrophotometric grade, 99+); B: Methanol 99.9%, Trifluoroacetic acid 0.1%. A Waters 996 PDA detector was used was used for UV-VIS signal detection over a wavelength range of 210-650 nm. with resolution of 1.2, and sampling rate of 1.0 spectrum/sec.

Mass spectrometry conditions: ion source parameters were as follows: capillary voltage 3200 V, sample cone voltage 35 V, extraction cone voltage 3 V, source temperature 110°C and desolvation temperature 350°C. Transfer optics settings were as follows: rf lens 375 V, rf dc offset-1was set to 4.0 V, rf dc offset set to 3.0 V, aperture 1.0 V, acceleration 180.0 V, focus 4.0 V and steering 0.0 V. Analyzer settings were as follows: resolution was set to 7500 at m/z 800 Th, MCP (multi channel plate) detector 2650 V, ion energy 32.0 V, tube lens 18.0 V, grid-2 42.0 V, TOF flight tube 4578.0 V and reflectron 1813.0 V. Cone gas and desolvation gas were set to 15 and 660 L/hour,

respectively. Lock spray parameters were identical to sample setting parameters. Lock spray sampling frequency mode was set to 5.

Data files were acquired in continuum mode and spectra were stored from m/z 100 to 2300 with a 2.3 second scanning cycle consisting of a 2.2 second data scan and a 0.1 second inter-scan delay. The pusher cycle time was set to 75 µs. TOF Calibration and Lock-Mass set up used a Lt_{eff} (effective length of the flight tube) value of 1124.8000 using the molecular ion signal of the Leucine Enkephalin at m/z = 556.2771 Th. System calibration was performed using Poly-D-L-alanine (P9003, Sigma, MO, USA); a 50 ng/mL solution of Leucine Enkephalin (L9133, Sigma, MO, USA) was infused at 5 µL/min into the lock spray (positive ion lock mass: 556.2771 Th) using an ISCO µLC-500 micro flow pump (The Teledyne Technologies Company, Lincoln, NE, USA). Savitsky-Golay smoothing using a ± 4 channel window was repeated twice and centered using the center at the 80% peak height to obtain accurate masses. After data acquisition and signal averaging, spectra were individually corrected relative to the Leucine Enkephalin lock-mass calibration mass via standard procedure (MassLynx 4.0 sp2 software/ Mass Measure).

To get accurate mass measurements raw data were corrected with lock mass in all the cases. To identify given protein components a library was created with all the known crystallins and possible modifications as independent variables (PTM) [68]. MassLynx 4.0 sp2 software (Waters/Micromass Manchester, UK) was used for instrument control, data acquisition and data evaluation.

3. Results

3.1 ^{14}C levels of water-soluble and water-insoluble proteins from lens nuclei

Lens nuclei isolated from 16 lenses from 12 different subjects were separated into water-soluble and water-insoluble components and analyzed for ^{14}C levels. Table 1 presents the ^{14}C concentration for these 16 nuclei and is reported in $F^{14}C$ and $\Delta^{14}C$ nomenclature. For every sample examined, the water-soluble fraction possessed a $F^{14}C$ value greater than the water-insoluble fraction. Many of these $F^{14}C$ values were only present in the atmosphere after the above ground testing of nuclear weapons occurred, which was well after the birth date of many of these subjects. The water-insoluble proteins maintain the lower levels of ^{14}C present around the time of birth of the fetal nuclei. The shaved lenses had some younger cells from the outer edges of the slices, however, and consequently had slightly higher $F^{14}C$ than the peeled lenses. The difference in $F^{14}C$ between water-soluble and water-insoluble paired samples was similar for each dissection method.

To estimate the amount of turnover that occurred in the water-soluble protein fraction compared to the water-insoluble fraction, the difference in log isotope ratios for the two fractions was examined. For the data from the lens nuclei from donors born before the start of the bomb pulse (before 1955) in Table 1, the difference in the log isotope ratios (IR), $\log(IR_{soluble}) - \log(IR_{insoluble}) = \log(IR_{soluble}/IR_{insoluble})$, was always positive, and the one sample t-test had a t-statistics of 8.6689 for 14 degrees freedom for a p-value of 0.00000053. The 95% confidence interval for the difference was (0.0453, 0.0717) indicating that the isotope ratio of the water-soluble fraction is at least 4-5% larger than in the insoluble fraction.

3.2 ^{14}C levels of water-soluble and water-insoluble proteins from layers of topologically stratified fiber cells from lenses

Layers of topologically stratified fiber cells from adult human cadaver lenses were removed incrementally using the water peeling method, enabling the isolation of similarly aged populations of fiber cells. From these cells the water-soluble and -insoluble proteins were isolated and AMS was used to determine the ^{14}C levels present in the water-soluble and water-insoluble proteins isolated from each of these cell layers. Figure 2 shows $^{14}C/C$ concentration reported in $F^{14}C$ units of the water-soluble and water-insoluble proteins isolated from the subjects born in 1933 (A) and 1962 (B), and where they fall along the atmospheric record for ^{14}C. For both donors the $F^{14}C$ for the water-insoluble proteins from the inner most (oldest) layer corresponds to the atmospheric level of ^{14}C present in the atmosphere at the subjects' date of birth. The ^{14}C level in the insoluble protein fraction relates to the average birthdate of the cells in that sample and was used to map the water-soluble data to the appropriate location on the bomb curve (i.e., the ^{14}C level of water-insoluble fraction anchors the chronological location on the bomb curve). Along the curve the ^{14}C level of the water-soluble fraction from each sample is plotted above or below the established average birthdate as determined by the water-insoluble fraction of the whole cells from which it was derived.

For the donor born in 1933 (Figure 2A) the inner six (oldest) layers display water-soluble fractions with higher $F^{14}C$ values than their water-insoluble counterparts. Higher $F^{14}C$ values correspond to these water-soluble fractions containing younger carbon on average than their water-insoluble counterparts. The three outer (youngest) layers possess $F^{14}C$ values for the water-soluble protein lower than water-insoluble protein, which again corresponds to the water-soluble fractions containing younger carbon on average compared to their water-insoluble counterparts. The drift of the ^{14}C concentration away from the levels established on the cells' birthday is due to inclusion or incorporation of newer carbon over the course of the donor's lifetime. New carbon incorporation in cells formed prior to the bomb pulse is not perceivable until 1955, and is

always observed as an increase in $^{14}C/C$ concentration above the atmospheric record. New carbon incorporation for cells born after the peak of the bomb pulse in 1963 is always observed as a decrease in $^{14}C/C$ concentration. The offset in the radiocarbon signature between the water-soluble and water-insoluble fractions allows for the quantification of the extent to which carbon turnover has occurred. For the donor born in 1962 (Figure 2B) when above ground testing of nuclear weapons was still occurring, cells from infancy can experience years of both higher or lower atmospheric levels of $^{14}CO_2$. The addition of new cellular carbon may initially increase and then later decrease the average $^{14}C/C$ concentration with respect to its concentration at birth.

Table 2 lists the $^{14}C/C$ concentration reported in $F^{14}C$ and $\Delta^{14}C$ units for the water-soluble and water-insoluble proteins from layers of topologically stratified fiber cells from 3 additional adult human cadaver lenses. Layers are numbered with 1 representing the outermost layer. In the case of the lens of the donor born in 1953, above ground testing of nuclear weapons had started but the atmosphere did not reflect the anthropogenic ^{14}C until 1955. Similar to the lens depicted in Figure 2B, cells born when the donor was a child during the period when testing was occurring can experience later years of both higher or lower atmospheric levels of $^{14}CO_2$. The addition of new cellular carbon may initially increase and then later decrease the average $^{14}C/C$ concentration of proteins.

The other two lenses in Table 2 are from individuals born before the bomb pulse. The inner layers of the lens contain the oldest synthesized proteins, yet the $F^{14}C$ for the water-soluble fraction is greater than that of the water-insoluble proteins, which indicates the incorporation of younger (bomb elevated) ^{14}C in these cells born prior to atmospheric testing of nuclear weapons. All carbon incorporated into existing lens cells after 1955 has a higher $F^{14}C$ than that in the water-insoluble fractions of those cells The

outer layers of the lens contain the younger cells formed after 1963. . The carbon added to these cells after their formation will always have a lower F14C. In cells born after the peak of the bomb pulse (1963), the water-soluble fractions possessing lower $F^{14}C$ than the paired water-insoluble fractions indicates new carbon incorporation in those cells.

3.3 Proteins identified in the water-insoluble fractions

The proteins present in the water-insoluble fraction of the lens were identified using LC-MS/MS. Table 3 presents the proteins identified in the water-insoluble fractions from the cadaver lenses. Two major categories of proteins were identified in the water-insoluble fraction, (1) crystallins and (2) membrane and cytoskeletal proteins. The method of protein identification included digest and solubilisation for LC, which also causes modifications, The water-insoluble fractions had much less mass than the water-soluble fractions. Material was not always available for protein MS for small water-insoluble samples because all the carbon was needed for isotope analyses. The list of modifications of the crystallins in Table 3 is not exhaustive, but includes the most common identified modifications.

3.4 Proteins identified in the water-soluble fractions

Proteins present in the water-soluble fraction of the lens were identified using HR LC-MS. Table 4 presents the proteins identified in the water-soluble fractions from the cadaver lenses. The proteins identified in the water-soluble fractions were all crystallins and harbored a variety of modifications. The list in Table 4 contains the majority of proteins accounting for the carbon mass associated with the isotopic measurements, it is not an exhaustive list of all proteins detected.

4.0 Discussion

The transport and circulation of water, electrolytes and small molecules within the lens is well documented and believed necessary for lens health [1,13,14,15, 26]. This circulation is both transverse, spanning layers of cells of different ages, and concentric, among layers of cells of the same age. A large molecule diffusion pathway (LMDP) distinct from gap junctions has also been described in the literature [27-29]. This pathway is primarily between cells of the same age and has been demonstrated using fluorescent proteins in mice and chickens, transverse transport of proteins among cells of different ages was very low over the short spans of observation [27-29]. The transport of young carbon in protein synthesized by cortical fiber cells to the deeper nuclear fiber cells via the LMDP may account for the observed 4-5% difference in $^{14}C/C$ observed between water-soluble and water-insoluble proteins of the lens nuclei.

The first direct evidence for *in vivo* carbon transport and turnover in adult human nuclear fiber cells is identified by using the chronologically-variable level of ^{14}C introduced to the atmosphere by above ground nuclear weapons testing from 1955-1963 [35-37]. This turnover occurs in the water-soluble proteins of the fiber cells. Our key finding is the discovery of an influx of new carbon within even the oldest fiber cells of the human eye lens. This water-soluble carbon was from a protein fraction identified as containing crystallin protein in the mass range of 19.5 kDa to 21.5 kDa. This is the first identification of *in vivo* carbon turnover in protein from human nuclear fiber cells, and contradicts the prevailing paradigm that carbon turnover does not occur in this region of the lens. In a study exploring the lens as a tissue for forensic dating, lens nuclei were surgically extracted and dated as whole tissue [49]. Although the authors stated there was no protein turnover, they did not isolate proteins and their data also clearly show new carbon in the lens nuclei [49].

It is reasonable that peptide or amino acid transport mechanisms are bi-directional so carbon can be transported radially in both directions. New carbon can move from outer young cells to inner old cells and old peptides can move from inner old cells toward younger cells on the outer layers of the lens. Based on our limited data there is a hint that peptides (or amino acids) are recycled from older regions of the lens back into the cortex. The 1989 data pair from the healthy 42-year old lens in Fig 2B exhibits a level of water-soluble ^{14}C that is elevated above subsequent atmospheric levels. The likely source of this material would be from deeper within the tissue itself or variability in the cell layers removed in the peeling dissection method. This recycling, not readily observable in the older lenses we examined, may be evidence that transport of materials between the cortex and the nucleus attenuates with age, which agrees with prior findings [4,16].

The younger carbon measured in the lens nuclei may also be a product of protein synthesis or repair from transported smaller molecules. It is difficult, however, to devise a mechanism by which protein synthesis could occur in the nucleus. Yet, our finding of younger carbon in water-soluble proteins of the nucleus is consistent with a study where poly(A)+mRNA was recovered and purified from bovine nuclear fiber cells and found to synthesize a protein profile distinct from that expressed in the lens cortical cells [69]. The profile was comprised predominantly of the crystallin proteins and was distinctly lacking in the expression of the higher molecular mass membrane and cytoskeletal proteins. Our data are consistent with these findings and suggest there could be a mechanism of small molecule transport combined with on-sight synthesis or repair of crystallin protein in nuclear fiber cells Our findings additionally show that human lens nuclei do not behave in a manner consistent with a syncytium as observed in chickens and mice [27,28]. Had the lens nuclei behaved as a true syncytium the nucleus would have exhibited a significantly more homogenous distribution of ^{14}C.

Although recycling of carbon within the lens complicates our ability to accurately quantify the total degree of carbon turnover in these cells, models can be constructed to estimate the degree of carbon turnover by using the atmospheric ^{14}C record and the paired data. Carbon turnover implies replacement of old carbon with new while keeping the total carbon inventory constant. The cycling carbon could be contained in whole proteins, peptides, amino acids, or other carbonaceous compounds. Models were constructed to account for the turnover of carbon.

One model assumes annual replacement of carbon with no physiological preference in which carbon atoms are replaced, any carbon atom in a population was equally likely to turnover each year. For example, if a tissue has 1% annual carbon turnover, 99% of the carbon is unchanged and 1% of the carbon gets the next year's $F^{14}C$ ratio from the published annual growing season average (zero turnover). The new total $F^{14}C$ is calculated and the process is repeated annually to produce the curves with different turnover rates (Figure 3). Carbon from subjects born before 1955 always possesses an increased $F^{14}C$ compared to their birth level if molecular turnover occurs during the time of the bomb pulse. Carbon from subjects born on the rise of the pulse (1955-1963) can exhibit an increased or decreased $F^{14}C$ depending on the rate of turnover and where they fall on the curve. Carbon from subjects born after the pulse always exhibits a decreased $F^{14}C$ if molecular turnover occurs because the newer carbon always has a lower $F^{14}C$ after the peak in 1963. If a small population of carbon molecules undergoes turnover in a primarily static pool, the deviation from zero turnover can be small [70]. The offset between paired protein samples in Figure 2A is consistent with 1-2% annual turnover of carbon between synthesis and date of death. Using this constant annual turnover model we estimate that the water-soluble carbon turns over at a rate of ~1% per year while the annual turnover of insoluble protein carbon was 0.0 – 0.1% (Figure 3). This nominal shift of water-insoluble ^{14}C may be due to formerly

soluble crystallins from a more modern time becoming insoluble after modification or oxidative damage, or perhaps precipitation (rather than turnover) since the water-insoluble carbon inventory increases.

The development of the cortical barrier makes the lifetime turnover scenario unlikely, however, so another model that assumed constant annual turnover during the first 40 years of life followed by complete cessation was examined. The 4-5% elevation of water-soluble $F^{14}C$ compared to its paired water-insoluble fraction is consistent with 0.5-1.0% annual carbon turnover exclusively during the first 40 years of life of the pre-1955 lens nuclei listed in Table 1. The 42 year-old lens from Table 1 can not be fit with this turnover rate, it needs ~2-3% annual carbon turnover for 40 years to fit the data to the ^{14}C record. This higher rate does not fit any of the other lenses, however, and suggests that the rate of new carbon incorporation likely varies with age.

The observed level of ^{14}C in the water-insoluble proteins for each layer isolated is consistent with a lack of new membrane/cytoskeletal protein incorporation and suggests that the insolublized (formerly soluble) crystallin protein observed in the insoluble fractions is a relic from the original cellular material. These proteins preserve their original levels of ^{14}C for over 50 years and serve as internal controls for determining the birth date of the population of cells from which they originate. The absence of bomb carbon in the nuclei of peeled lenses demonstrates that our dissection protocols yielded cellular material in a uniform fashion without significant mixing of older and younger regions of the lens. Exhibiting minimal (if any) turnover, the ^{14}C level of water-insoluble protein can provide an approximate “birthday” of the parent cells through correlation with the atmospheric $^{14}CO_2$ record as depicted in the bomb pulse (Fig 2A). This ascribed date represents an average birthday that spans multiple layers of fibers that were removed concomitantly. With the exception of the nucleus that develops during

gestation, we do not have a means to determine the exact time of synthesis of these cells. However, as can be seen in Fig 2B (a lens from a donor born in 1962) we are indeed capable of dating the nucleus to precisely the calendar year these cells were formed.

Cataracts are the leading cause of blindness worldwide and are associated with extensive protein oxidation and insolubility. There has yet to be an answer as to why half the U.S. population over 65 experiences cataracts [71], but we may be one step closer in our understanding as to why the other half in the U.S. do not develop cataracts. We now know that the incorporation of new carbon into crystallin protein is a regular physiological process of our oldest lens cells. It may well be true that ARN cataracts arise (at least in part) by attenuation or loss of protein repair or transport mechanisms. If this is indeed the case, therapy for the resuscitation of these mechanisms could alleviate or postpone the need for cataract surgery and save billions of dollars annually for the U.S. Medicare System and healthcare industries of Western Europe and Australia [71].

Acknowledgements

Support for DNS was provided by the LLNL Center for Accelerator Mass Spectrometry minigrant program and the LLNL UEPP Program. BDH is a George and Judy Marcus Senior Fellow of the American Asthma Society. The authors wish to thank the individuals who donated their bodies and tissues for the advancement of education and research, which were provided by the UC Anatomical Materials Programs. We thank Charlotte Wacker for assistance in acquiring lenses, Lucille Ngai, Michelle Hoyt, and Nguyen Nguyen for assistance in processing samples, and Paula Zermeño for preparing AMS samples for measurement. Support was provided by NIEHS P42ES004699, NIEHS R01ES002710, NIH/NCRR 5P41RR013461, NIGMS

8P41GM103483, NIH/NCRR RR024146, NIH/NHGRI HG003352, NIH/NEI EY018722, EY08747 and LLNL LDRD 10-LW-033. The content is solely the responsibility of the authors and does not necessarily represent the official views of the National Institute of Environmental Health Sciences or the National Institutes of Health. This work was performed in part under the auspices of the U.S. Department of Energy by Lawrence Livermore National Laboratory under Contract DE-AC52-07NA27344.

References

1. Beebe DC. "The Lens," in Kaufman PL, Alm A. (Eds.), Adler's Physiology of the Eye, Clinical Applications 10th Ed., Mosby, Inc., St. Louis, MO USA 2003; pp. 117-158.
2. Taylor VL, Al-Ghoul KJ, Lane CW, Davis VA, Kuszak JR, Costello MJ. Morphology of the normal human lens. Invest. Ophthalmol. Vis. Sci. 1996; 37:1396-1410.
3. Bloemendal H, de Jong W, Jaenicke R, Lubsen NH, Slingsby C, Tardieu A. Ageing and vision: structure, stability, and function of lens crystalline. Prog. In Biophysics & Mol. Bio. 2004; 86:407-85.
4. Truscott RJW. Age-related nuclear cataract—oxidation is the key. Exp. Eye Res. 2005; 80:709-25.
5. Friedrich MG, Truscott RJW. Large-scale Binding of α-crystallin to cell membranes of aged normal human lenses: a phenomenon that can be induced by mild thermal stress. Invest Ophthalmol Vis Sci 2010; 51:5145-5152.
6. Truscott RJW, Zhu X. Presbyopia and cataract: a question of heat and time. Prog. Retinal and Eye Res 2010; 29:487-99.
7. Hains PG, Truscott RJW. Age-dependent deamidation of lifelong proteins in the human lens. Invest Ophthalmol Vis Sci 2010; 51:3107-3114.
8. Zhu X, Gaus K, Lu Y, Magenau A, Turscott RJW, Mitchell TW. α- and β-Crystallins modulate the head group order of human lens membranes during aging. Invest Ophthalmol Vis Sci 2010; 51:5162-5167.
9. Su S, McArthur JD, Truscott RJW, Aquilina JA. Truncation, cross-linking and interaction of crystallins and intermediate filament proteins in the aging human lens. Biochemica et Biophysica Acta 2011; 1814:647-656.
10. Truscott RJW, Comte-Walters S, Ablonczy Z, Schwacke JH, Berry Y, Korlimbinis A, Friedrich MG, Schey KL. Tight binding of proteins to membranes from older human cells. AGE 2011; 33:543-554.
11. Robinson ML, Lovicu FJ. The Lens: Historical and Comparative Perspectives, in: Lovicu FJ & Robinson ML (Eds), Development of the Ocular Lens. Cambridge University Press, New York, 2004; pp 3-26.

12. Berthoud VM, Beyer EC. Oxidative stress, lens gap junctions, and cataracts. Antioxid Redox Signal 2009; 11:339-53.
13. Mathias RT, Rae JL. The lens: local transport and global transparency. Exp. Eye Res. 2004; 78:689–98.
14. Mathias RT, Kistler J, Donaldson P. The lens circulation. J Membrane Biol 2007; 216:1-16.
15. Vaghefi E, Pontre B, Donaldson PJ, Hunter PJ, Jacobs MD. Visualization of transverse diffusion paths across fiber cells of the ocular lens by small animal MRI. Physiol. Meas. 2009; 30:1061-1073.
16. Mathias RT, White TW, Gong X. Lens gap junctions in growth differentiation and homeostasis. Physiol. Rev. 2010; 90:179-206.
17. Dahm R, van Marle J, Quinlan RA, Prescott AR, Vrensen GFJM. Homeostasis in the vertebrate lens: mechanisms of solute exchange. Phil. Trans. R. Soc. B 2011; 366:1265-1277.
18. Vaghefi E, Walker K, Pontre BP, Jacobs MD, Donaldson PJ. Magnetic resonance and confocal imaging of solute penetration into the lens reveals a zone of restricted extracellular space diffusion. Am J Physiol. Regulatory, integrative and comparative physiol 2012; 302:R1250-R1259.
19. Shiels A, Bassnett S. Mutations in the founder of the MIP gene family underlie cataract development in the mouse. Nature Genet. 1996; 12:212-5.
20. Berry V, Francis P, Kaushal S, Moore A, Bhattacharata S. Missense mutations in MIP underlie autosomal dominant ‘polymorphic’ and lamellar cataracts linked to 12q. Nat. Genet. 2000; 25:15-7.
21. Ball LE, Garland DL, Crouch RK, Schey KL. Post-translational modifications of aquaporin 0 (AQP0) in the normal human lens: spatial and temporal occurrence. Biochem. 2004; 43:9856-65.
22. Fleschner C, Cenedella R. Lipid composition of lens plasma membrane fractions enriched in fiber junctions. J. Lipid Res. 1991; 32:45-53.
23. Mangenot S, Buzhynskyy N, Girmens J, Scheuring S. Malformation of junction microdomains in cataract lens membranes from a type II diabetes patient. Pflugers. Arch. – Eur. J. Physiol. 2009; 457:1265-74.

24. Fan J, Donovan AK, Ledee DR, Zelenka PS, Fariss RN, Chepelinsky AB. Gamma E-crystallin recruitment to the plasma membrane by specific interaction between lens MIP/aquaporin-0 and gammaE-crystallin. Invest. Opthalmol. Vis. Sci. 2004; 49:511-21.
25. Dorsaz N, Thurston GM, Stradner A, Schurtenberger P, Foffi G. Colloidal characterization and thermodynamic stability of binary eye lens protein mixtures. J. Phys. Chem. B 2009; 113:1693-1709.
26. Truscott RJW. Age-related nuclear cataract: A lens transport problem. Ophthalmic Res. 2000; 32:185-94.
27. Shestopalov VI, Bassnett S. Expression of autofluorescent proteins reveals a novel protein permeable pathway between cells in the lens core. J. Cell Sci. 2000; 113:1913-21.
28. Shestopalov VI, Bassnett S. Development of a macromolecular diffusion pathway in the lens. J. Cell Sci. 2003; 116:4191-9.
29. Shi Y, Barton K, De Maria A, Petrash M, Shiels A, Bassnett S. The stratified syncytium of the vertebrate lens. J. Cell Sci. 2009; 122:1607-15.
30. Young RW, Fulhorst HW. Regional differences in protein synthesis within the lens of the rat. Invest. Opththalmol. 1966; 5:288-97.
31. De Vries H. Atomic bomb effect: variation of radiocarbon in plants, shells, and snails in the past 4 years. Science 1958; 128:250-1.
32. Nydal R, Lovseth K. Distribution of radiocarbon from nuclear tests. Nature 1965; 206:1029-31.
33. Stuiver M, Reimer PJ, Baziunas TF. High-precision radiocarbon age calibration for terrestrial and marine samples. Radiocarbon 1998; 40:1127-51.
34. Levin I, Kromer B. The tropospheric $^{14}CO_2$ level in mid latitudes of the northern hemisphere (1959-2003). Radiocarbon 2004; 46:1261-72.
35. Hua Q, Barbetti M. Review of tropospheric bomb ^{14}C data for carbon cycle modeling and age calibration purposes. Radiocarbon 2004; 46:1273-98.
36. Graven HD, Guilderson TP, Keeling RF. Observations of radiocarbon in CO_2 at La Jolla, California, USA 1992-2007: Analysis of the long-term trend. J. Geophysical Research 2012; 117:D02302.

37. Levin I, Naegler T, Kromer B, Diehl M, Francey RJ, Gomez-Pelaez AJ, Steele LP, Wagenbach D, Weller R, Worthy DE. Observations and modelling of the global distribution and long-term trend of atmospheric $^{14}CO_2$. Tellus 2010; 62B:26-46.
38. Harkness DD. Further investigations of the transfer of bomb ^{14}C to man, Nature 1972; 240:302-3.
39. Libby WF, Berger R, Mead JF, Alexander GV, Ross JF. Replacement rates for human tissue from atmospheric radiocarbon. Science 1964; 146:1170-2.
40. Harkness DD, Walton A. Carbon-14 in the biosphere and humans. Nature 1969; 223:1216-8.
41. Shapiro SD, Endicott SK, Province MA, Pierce JA, Campbell EJ. Marked longevity of human lung parenchymal elastic fibers deduced from prevalence of D-aspartate and nuclear-weapons related radiocarbon. J. Clinical Investigation 1991; 87:1828-34.
42. Wild EM, Arlamovsky KA, Golser R, Kutschera W, Priller A, Puchegger S, Rom W, Steier P, Vycudilik W. ^{14}C dating with the bomb peak: An application to forensic medicine. Nucl. Instrum. Methods Phys. Res. Sect. B 2000; 172:944-50.
43. Lovell MA, Robertson JD, Buchholz BA, Xie C, Markesbery WR. Use of bomb pulse carbon-14 to age senile plaques and neurofibrillary tangles in the Alzheimer's Disease brain. Neurobiology of Aging 2002; 23:179-86.
44. Spalding KL, Bhardwaj RD, Buchholz BA, Druid H, Frisén J. Retrospective birth dating of cells. Cell 2005; 122:33-43.
45. Spalding KL, Buchholz BA, Druid H, Bergman L, Frisén J. Forensic medicine: age written in teeth by nuclear bomb tests. Nature 2005; 437:333-4.
46. Ubelaker DH, Buchholz BA, Stewart J. Analysis of artificial radiocarbon in different skeletal and dental tissue types to evaluate date of death. J. Forensic Sciences 2006; 51:484-8.
47. Bhardwaj RD, Curtis MA, Spalding KL, Buchholz BA, Fink D, Bjork-Eriksson T, Nordborg C, Gage FH, Druid H, Eriksson PS, Frisén J. Neocortical neurogenesis in humans is restricted to development. Proc. Natl. Acad. Sci. USA 2006; 103:12564–8.

48. Spalding KL, Arner E, Westermark PO, Bernard S, Buchholz BA, Bergman OI, Blomqvist L, Hoffstedt J, Näslund JE, Britton T, Concha H, Hassan M, Rydén M, Frisén J, Arner P. Dynamics of fat cell turnover in humans. Nature 2008; 453:783-7.
49. Lynnerup N, Kjeldsen H, Heegaard S, Jacobsen C, Heinemeier J. Radiocarbon dating of the human eye lens crystallines reveal proteins without carbon turnover throughout life. PLoS ONE 2008: 3:e1529. doi:10.1371/journal.pone.0001529.
50. Bergmann O, Bhardwaj RD, Bernard S, Zdunek S, Barnabé-Heider F, Walsh S, Zupicich J, Alkass K, Buchholz BA, Druid H, Jovinge S, Frisén. Evidence for cardiomyocyte renewal in humans. Science 2009; 324:98-102.
51. Alkass K, Buchholz BA, Ohtani S, Yamamoto T, Druid H, Spalding KL. Age estimation in forensic sciences: Application of combined aspartic acid racemization and radiocarbon analysis. Mol Cell Proteomics 2010; 9:1022-30.
52. Buchholz BA, Spalding KL. Year of birth determination using radiocarbon dating of dental enamel. Surf. Interface Anal. 2010; 42:398-401.
53. Perl S, Kushner JA, Buchholz BA, Meeker AK, Stein GM, Hsieh M, Kirby M, Pechhold S, Liu EH, Harlan DM, Tisdale JF. Significant human beta-cell turnover is limited to the first three decades of life as determined by in-vivo thymidine analog incorporation and radiocarbon dating. J. Clin Endocrinol Metab. 2010; 95:E234-9.
54. Arner P, Bernard S , Salehpour M , Possnert G, Liebl J, Steier P, Buchholz BA, Eriksson M, Arner E, Hauner H, Skurk T, Rydén M, Frayn KN, Spalding KL. Dynamics of human adipose lipid turnover in health and metabolic disease. Nature 2011; 478:110-3.
55. Bergmann O, Liebl J, Bernard S, Alkass K, Yeung MSY, Steier P, Kutschera W, Johnson L , Landén M, Druid H, Spalding KL, Frisén J. The age of ofactory bulb neurons in humans. Neuron 2012; 74:634-9.
56. Hägg S, Salehpour M, Noori P, Lundström J, Possnert G, Takolander R, Konrad P, Rosfors S, Ruusalepp A, Skogsberg J, Tegnér J, Björkegren J. Carotid plaque age is a feature of plaque stability inversely related to levels of plasma insulin. PLoS ONE 2011; 6:e18248. doi:10.1371/journal.pone.0018248
57. Griess G, Zigman S, Yulo T. Modification of calf lens crystallins as determined by gel electrophoresis. Mol. Cell. Biochem. 1976; 12:9-14.

58. Cotlier E, Obara Y, Toftness B. Cholesterol and phospholipids in protein-fractions of human lens and senile cataract. Biochimica et Biophysics Acta 1978; 530:267-278.
59. Fleschner CN, Cenedella RJ. Lipid-composition of lens plasma-membrane fractions enriched in fiber junctions. J. Lipid Res. 1991; 32:45-53.
60. Mitchell J, Cenedella RJ. Human lens cholesterol concentrations in patients who used Lovastatin or Simvastatin. Arch Ophthalmol 1999; 117:653-657.
61. Jacob RF, Cenedella RJ, Mason RP. Direct evidence for immiscible cholesterol domains in human ocular lens fiber cell plasma membranes. J. Biol. Chem. 1999; 274:31613-31618.
62. Vogel JS, Southon JR, Nelson DE. Catalyst and binder effects in the use of filamentous graphite for AMS. Nucl. Instrum. Methods Phys. Res. Sect. B 1987; 29:50-6.
63. Santos GM, Southon JR, Druffel-Rodriguez KC, Griffin S, Mazon M. Magnesium perchlorate as an alternative water trap in AMS graphite sample preparation: A report on sample preparation at KCCAMS at the University of California, Irvine. Radiocarbon 2004; 46:165-73.
64. Brown TA, Southon JR. Corrections for contamination background in AMS ^{14}C measurements. Nucl. Instrum. Methods Phys. Res. Sect. B 1997; 123:208-13.
65. Scott EM. The Third International Radiocarbon Intercomparison (TIRI) and Fourth International Radiocarbon Intercomparions (FIRI) 1990-2002 results, analyses, and conclusions. Radiocarbon 2003; 45:135-408.
66. Reimer PJ, Brown TA, Reimer RW. Discussion: reporting and calibration of post-bomb ^{14}C data. Radiocarbon 2004; 46:1299-1304.
67. Stuiver M, Polach HA. Reporting of ^{14}C data. Radiocarbon 1977; 19:355-63.
68. Hoehenwater W, Klose J, Jungblut PR. Eye lens proteomics. Amino Acids 2006; 30:369-89.
69. Lieska N, Krotzer K, Yang H. A reassessment of protein synthesis by lens nuclear fiber cells. Exp. Eye Res. 1992; 54:807-11.
70. Falso MJS, Buchholz BA. Bomb pulse biology. Nucl. Instrum. Methods Phys. Res., Sect. B 2013; 294: 666-670.

71. American Medical Association Eye Diseases Prevalence Research Group. Prevalence of cataract and pseudophakia/aphakia among adults in the United States. Arch. Ophthalmol. 2004; 122:487-94.

Figure Legends

Figure 1. The ^{14}C bomb curve is recorded in biomolecules. Above ground nuclear testing nearly doubled the level of radiocarbon (as $^{14}CO_2$) in the atmosphere between 1955 and 1963. The atmospheric ^{14}C levels depicted by the dark blue trace are growing season averages for the northern hemisphere expressed in $F^{14}C$ units (fraction modern with $\delta^{13}C$ fractionation correction). These ^{14}C levels are recorded in annual plant growth and human diets. Human tissue incorporates the contemporary ^{14}C signature of their food at the time of synthesis. Years later specific biomolecules can be isolated and measured for ^{14}C content to establish carbon turnover or lack thereof, as in the cellulose of tree rings.

Figure 2. Water-soluble and -insoluble proteins from the same cells possess different ^{14}C signatures. Fiber cells from human cadaver lenses were peeled away in concentric layers to step back in time from the periphery (youngest) to the embryonic nucleus (oldest). Each fraction containing multiple layers of cells was centrifuged to separate soluble proteins (crystallins exclusively) from insoluble proteins (membrane, cytoskeleton, precipitated or insoluble crystallins). Data pairs along the atmospheric record (solid black line) represent the water-soluble and water-insoluble fractions from the same cohort of cells. Vertical lines denote the year of birth for each subject born in 1933 (A) and 1962 (B). The dashed horizontal line denotes the contemporary ^{14}C concentration in the atmosphere at the time of death. The insoluble fraction exhibits little or no carbon turnover and is correlated to the average “birthdate” of the group of cells. The insoluble fractions of the inner layers of the subject born in 1933 (A) do not contain any measurable new carbon while corresponding soluble fraction is skewed by the addition of more recent carbon in both subjects (A,B). The younger carbon in the soluble crystallins provides direct evidence of protein turnover. Error bars are smaller than the symbols, averaging ±0.005.

Figure 3. Annual carbon turnover changes the shape of the ^{14}C bomb curve. If turnover is less than 0.1% annually it is difficult to detect after the onset of the pulse. When turnover reaches 10% the pulse is almost completely flattened. The offsets of radiocarbon in the lenses fit a model suggesting ~0.01 turnover (1% annual).

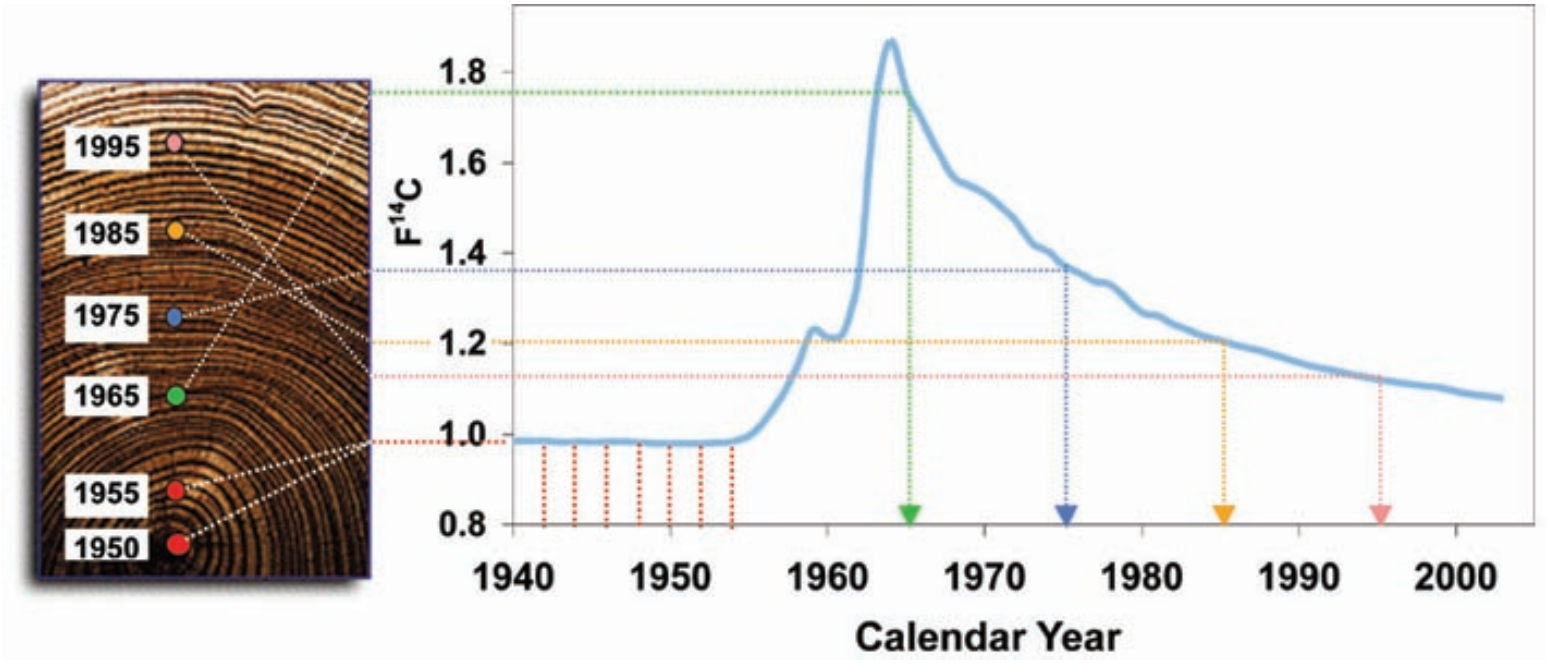
1995
1985
1975
1965
1955
1950
F14C
1.8
1.6
1.4
1.2
1.0
0.8
1940
1950
1960
1970
1980
1990
2000
Calendar Year

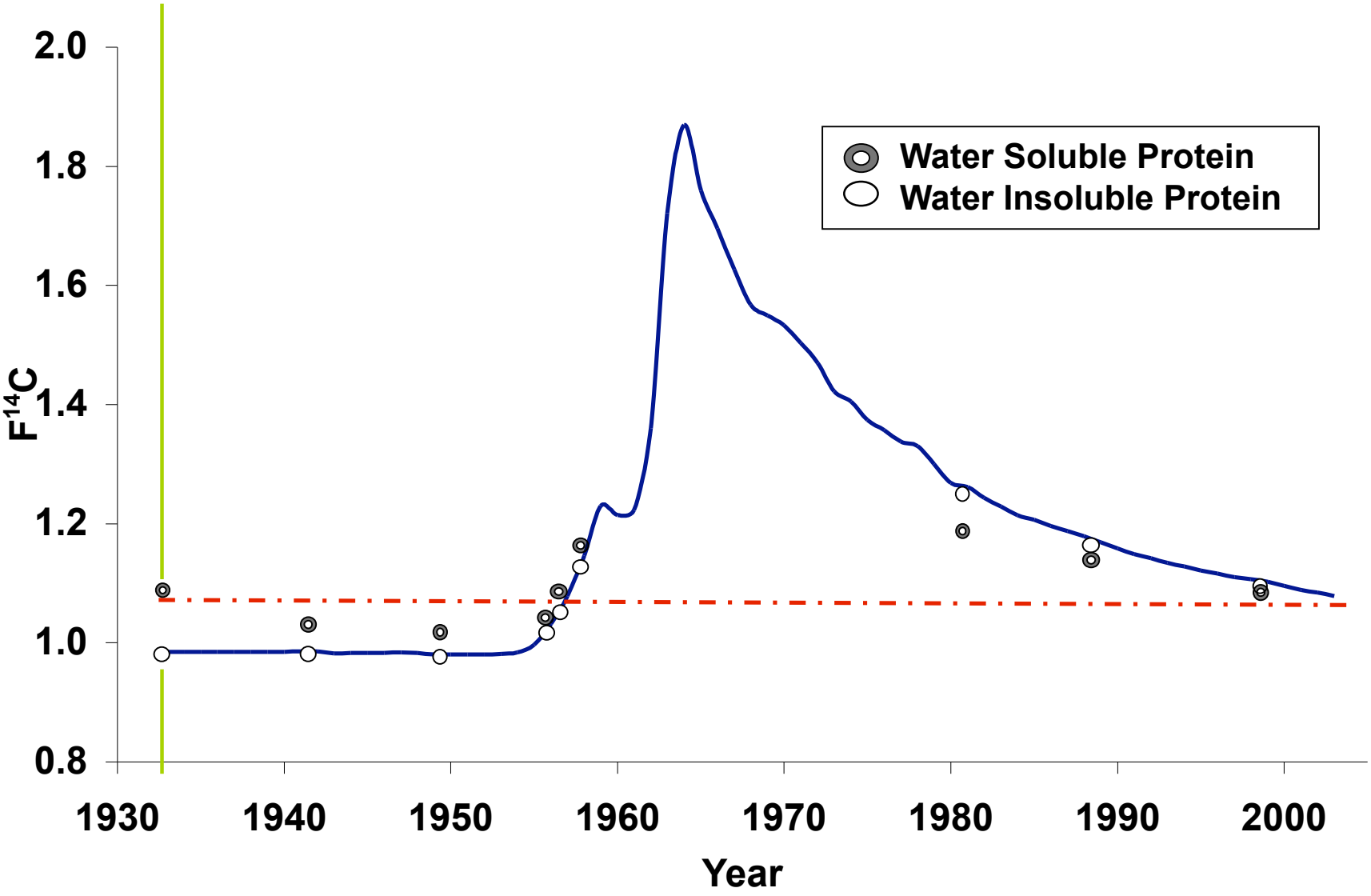
2.0
1.8
1.6
1.4
1.2
1.0
0.8
F14C
1930
1940
1950
1960
1970
1980
1990
2000
Year
Water Soluble Protein
Water Insoluble Protein

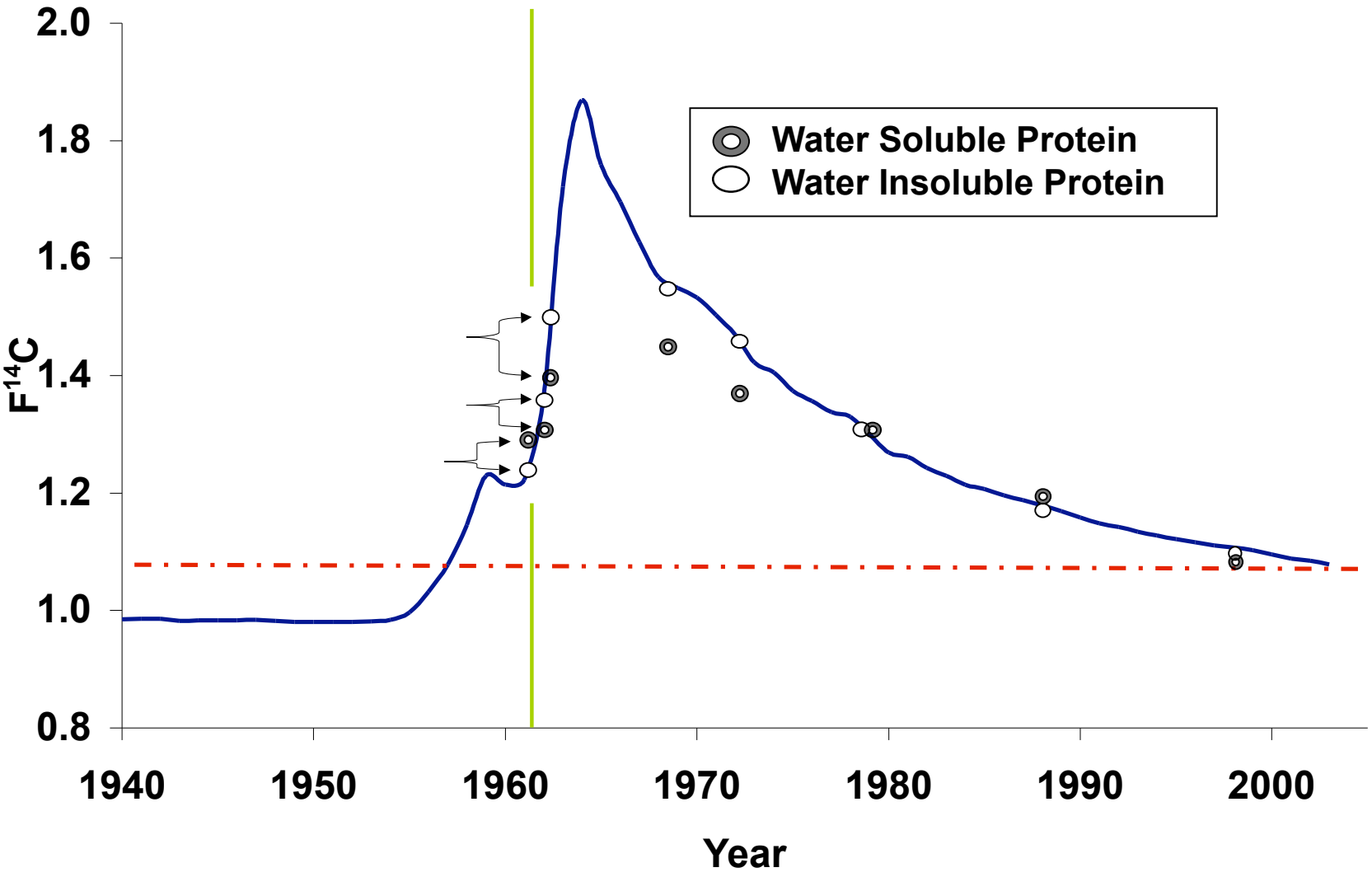
2.0
1.8
1.6
1.4
1.2
1.0
0.8
F14C
1940
1950
1960
1970
1980
1990
2000
Year
Water Soluble Protein
Water Insoluble Protein

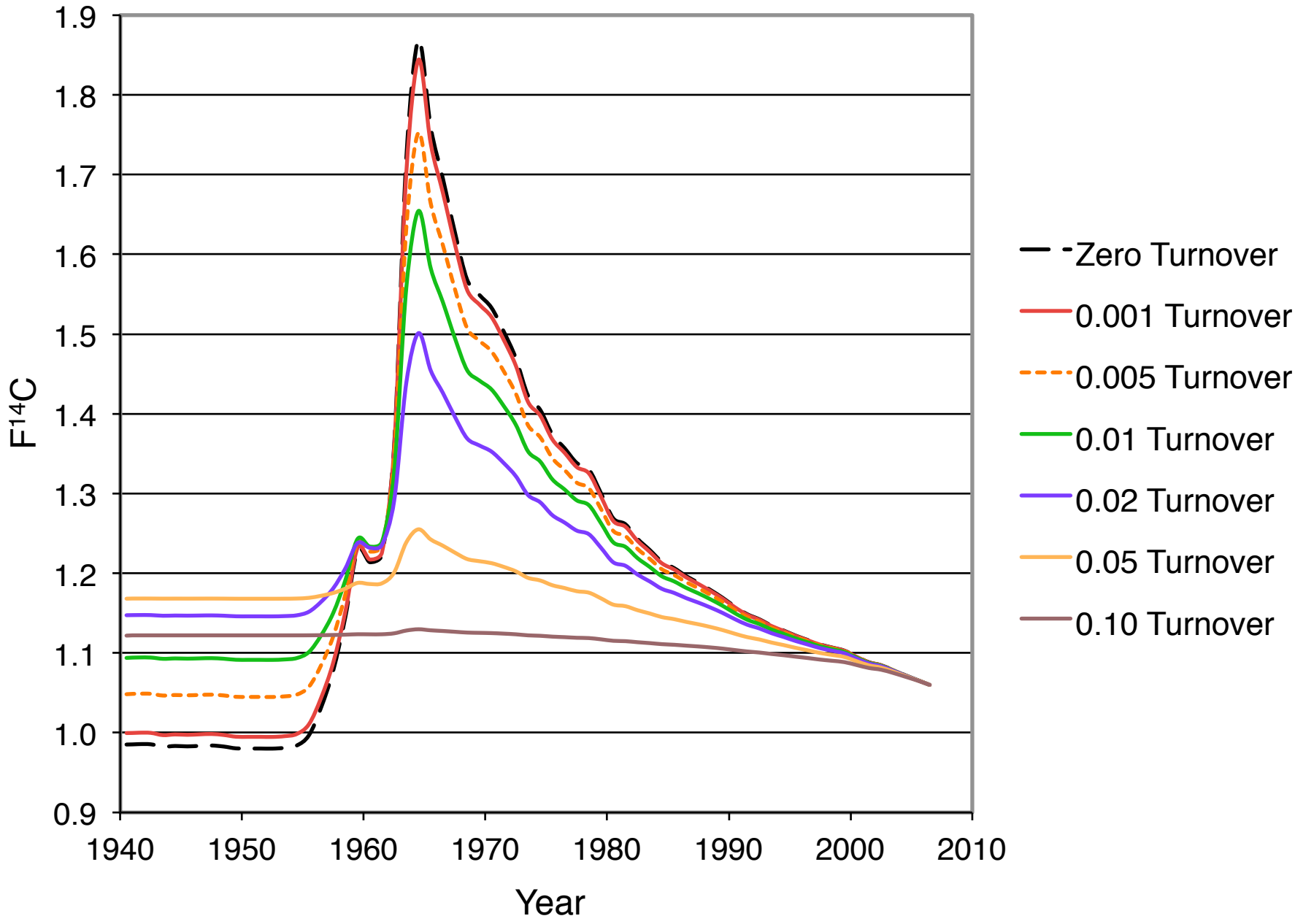
1.9
1.8
1.7
1.6
1.5
1.4
1.3
1.2
1.1
1.0
0.9
F14C
1940
1950
1960
1970
1980
1990
2000
2010
Year
Zero Turnover
0.001 Turnover
0.005 Turnover
0.01 Turnover
0.02 Turnover
0.05 Turnover
0.10 Turnover

Table 1. Lens Nuclei ^{14}C Data

Year of	Age	Water-soluble fraction				Water-insoluble fraction			
Death	(y)	$F^{14}C$	±[a]	$\Delta^{14}C$	±[a]	$F^{14}C$	±[a]	$\Delta^{14}C$	±[a]
2005	42	1.2942	0.0051	285.5	5.1	1.2217	0.0091	213.4	9.1
2005	65	1.1018	0.0042	94.5	4.2	1.0319	0.0039	25.1	3.9
2006	73	1.1027	0.0040	95.2	4.0	1.0158	0.0038	8.9	3.8
2006	53	1.0780	0.0039	70.7	3.9	1.0333	0.0046	26.3	4.6
2007	62	1.0298	0.0038	22.8	3.8	1.0002	0.0043	-6.6	4.3
2007	62	1.0623	0.0040	55.0	4.0	0.9946	0.0038	-12.3	3.8
2007	61	1.0581	0.0039	50.9	3.9	0.9557	0.0035	-50.9	3.5
2007	61	1.1038	0.0038	96.2	3.8	0.9980	0.0038	-8.9	3.8
2007	80	1.0325	0.0042	25.4	4.2	0.9934	0.0039	-13.4	3.9
2007	80	1.0675	0.0041	60.1	4.1	1.0017	0.0040	-5.1	4.0
2007	74	1.0385	0.0040	31.4	4.0	0.9890	0.0043	-17.7	4.3
2010	83	1.0229	0.0071	15.4	7.1	0.9850	0.0044	-22.3	4.4
2010	70	1.1045	0.0039	96.5	3.9	1.0521	0.0035	44.5	3.5
2010	82	1.0335	0.0036	25.9	3.6	1.0252	0.0031	17.7	3.1
2010	83	1.0759	0.0039	68.1	3.9	1.0100	0.0033	2.7	3.3
2010	83	1.1166	0.0039	116.6	3.9	1.0297	0.0037	22.3	3.9

[a]Uncertainties are ± 1 s.d.

Table 2. ^{14}C Data from Layers Peeled from Human Lenses

53 year old 1953-2006	Water-soluble				Water-insoluble			
Layer	$F^{14}C$	±	$\Delta^{14}C$	±	$F^{14}C$	±	$\Delta^{14}C$	±
1	1.0830	0.0038	75.7	3.8	1.0982	0.0036	90.8	3.6
2	1.1363	0.0038	128.6	3.8	1.1825	0.0044	174.5	4.4
3	1.2791	0.0051	270.4	5.1	1.3658	0.0052	356.6	5.2
4	1.2585	0.0053	250.0	5.3	1.3063	0.0059	297.5	5.9
5	1.1463	0.0041	138.6	4.1	1.0815	0.0045	74.2	4.5
6	1.1689	0.0048	161.0	4.8	na.	na.	na.	na
7	1.0780	0.0039	70.7	3.9	1.0333	0.0046	26.3	4.6
80 year old 1926-2007	Water-soluble				Water-insoluble			
Layer	$F^{14}C$	±	$\Delta^{14}C$	±	$F^{14}C$	±	$\Delta^{14}C$	±
1	1.1245	0.0039	116.8	3.9	1.1836	0.0042	175.4	4.2
2	1.1918	0.0040	183.6	4.0	1.2165	0.0041	208.1	4.1
3	1.0686	0.0036	61.2	3.6	1.0439	0.0033	36.7	3.3
4	1.0328	0.0037	25.7	3.7	0.9949	0.0041	-11.9	4.1
5	1.0251	0.0040	18.1	4.0	0.9999	0.0033	-7.0	3.3
6	1.0328	0.0034	25.7	3.4	0.9988	0.0033	-8.0	3.3
65 year old 1939-2005	Water-soluble				Water-insoluble			
Layer	$F^{14}C$	±	$\Delta^{14}C$	±	$F^{14}C$	±	$\Delta^{14}C$	±
1	1.1541	0.0044	146.4	4.4	1.2040	0.0065	196.0	6.5
2	1.1542	0.0051	146.5	5.1	1.2019	0.0049	193.9	4.9
3	1.2738	0.0049	265.4	4.9	1.2914	0.0051	282.8	5.1
4	1.2578	0.0047	249.4	4.7	1.2001	0.0058	192.1	5.8
5	1.1018	0.0042	94.5	4.2	1.0319	0.0039	25.1	3.9

Layer numbers are incremental, starting from the outer cortex/capsule (layer 1) and progressing inward to the nucleus. Uncertainties are ± 1 s.d. Sample marked na was not available due to loss during processing.

Table 3. Identified proteins of the water-insoluble fractions

Water-insoluble crystallins	Water-insoluble membrane and cytoskeletal proteins
α Crystallin A chain	Filensin
α Crystallin B chain	Phakinin
β Crystallin A2	Spectrin
β Crystallin A3	Actin
β Crystallin A4	Tubulin
β Crystallin B1	Fibrillin
β Crystallin B2	Keratin
β Crystallin B3	Vimentin
γ Crystallin S	Aquaporin-0 (AQP0)
γ Crystallin S	
γ Crystallin B	
γ Crystallin C	
γ Crystallin D	
Water-insoluble crystallins with modifications	
α Crystallin A chain	acetylation
α Crystallin A chain	2 x acetylation
α Crystallin A chain	Cysteine crosslink
α Crystallin A chain	Cysteine crosslink + acetylation
α Crystallin B chain	acetylation
α Crystallin B chain	acetylation + (sulphonation or phosphorylation)
α Crystallin B chain	acetylation + 2 x (sulphonation or phosphorylation)
α Crystallin B chain	sodiation

Table 4. Identified proteins of the water-soluble fractions

Protein	Observed Mass (Da)	Modification
α Crystallin A chain	19932.8	Sodiation
	19950.2	Acetylation
	19906.2	Cysteine crosslink
	19949.8	Cysteine crosslink + Acetylation
α Crystallin B chain	20180.4	Sodiation
	20200.2	Acetylation
	20221.6	Sodiation + Acetylation
	20242.3	2 x Acetylation
	20279.6	Acetylation + Sulphonation or phosphorylation
	20360.8	Acetylation + dual Sulphonation and or phosphorylation
γ Crystallin C chain	20878.8	none
γ Crystallin S chain	21005.0	none